Biosensors and Bioelectronics xxx (xxxx) 113961

Contents lists available at ScienceDirect

Biosensors and Bioelectronics

journal homepage: www.elsevier.com/locate/bios

Sensitive and real-time detection of IgG using novel interferometric reflecting imaging sensor system

Monireh Bakhshpour [a, b], Elisa Chiodi [b], Iris Celebi [b], Yeşeren Saylan [a], Nese Lortlar Ünlü [c], M. Selim Ünlü [b, c], Adil Denizli [a, *]

[a] Hacettepe University, Department of Chemistry, Ankara, Turkey
[b] Boston University, Department of Electrical and Computer Engineering, Boston, MA, United States
[c] Boston University, Department of Biomedical Engineering, Boston, MA, United States

ARTICLE INFO

Keywords:
Immunoglobulin G
Interferometric reflecting imaging sensor
Medical applications
Real-time detection

ABSTRACT

Considering the limitations of well-known traditional detection techniques, innovative research studies have focused on the development of new sensors to offer label-free, highly sensitive, real-time, low-cost, and rapid detection for biomolecular interactions. In this study, we demonstrate immunoglobulin G (IgG) detection in aqueous solutions by using real-time and label-free kinetic measurements of the Interferometric Reflectance Imaging Sensor (IRIS) system. By performing kinetic characterization experiments, the sensor's performance is comprehensively evaluated and a high correlation coefficient value (>0.94) is obtained in the IgG concentration range of 1–50 μg/mL with a low detection limit (0.25 μg/mL or 1.67 nM). Moreover, the highly sensitive imaging system ensures accurate quantification and reliable validation of recorded binding events, offering new perspectives in terms of direct biomarker detection for clinical applications.

1. Introduction

Glycoproteins are widely used as diagnostic biomarkers for critical diseases in many medical application platforms (Chen et al., 2012). Immunoglobulins as glycoproteins can bind to self-producing active antigens as a result of immune system response (Vidarsson et al., 2014). The role and importance of immunoglobulins for *in vivo* diagnostic research is increasing rapidly. Immunoglobulin gamma (IgG), the most abundant type of antibody (Bashal, 2013; Saylan et al., 2014a), represents 75–80% of all immunoglobulins in serum and is found in all body fluids. Therefore, IgG plays a crucial role in the immune system, against bacterial, and viral infections and also the anti-infective immunity in newborns as it can cross the placenta barrier. Moreover, the level of IgG in blood increases with certain disorders such as systemic lupus erythematosus, and hyperthyroidism (Hou et al., 2020; Kobayashi et al., 2013; Saylan et al., 2014b). As another example of its significance, a convenient way to determine the presence of the novel coronavirus in the human body is to detect the presence of relevant IgG in the bloodstream, as it persists longer than recombinant viral antigens (Younes et al., 2020). The expression of IgG antibodies in the body is the first response for most infectious diseases, hence, IgG detection has significant importance in the field of medical applications such as drug development and quality control, and diagnostic areas (Peeling et al., 2010; Bakhshpour et al., 2016).

For this reason, investigating the binding thoroughly between the receptor and ligand is crucial for IgG detection and characterization. As a matter of fact, studying the ligand-target interaction provides information regarding the nature of biochemical reactions that define a specific biological function. Specifically, the affinity between IgG and protein A, one of the several virulence factors of *Staphylococcus aureus,* was demonstrated in the literature by using enzyme-linked immunosorbent assay (ELISA) and agglutination test systems (Yu et al., 2016). However, despite their popularity in the biomedical research field, such assays are cumbersome, time-consuming, and expensive. Moreover, current ELISA methods feature multiple challenging steps, such as effective labeling, as well as the usage of low-affinity, highly monoclonal antibody-antigen pairs due to the need to target multiple isotopes. These issues can sometimes be a deterrent for large-scale applications (Inci et al., 2020).

Recently, label-free sensors have been applied to the detection of IgG with different modalities including optical, electrochemical, and piezoelectric (Bakhshpour et al., 2017; Divya and Dharuman, 2021; Tran et al., 2020). Particularly, the interferometric reflecting imaging sensor (IRIS) system has been chosen to carry out the experiments de-

* Corresponding author.
E-mail address: denizli@hacettepe.edu.tr (A. Denizli).

https://doi.org/10.1016/j.bios.2021.113961
Received 11 November 2021; Received in revised form 20 December 2021; Accepted 31 December 2021
0956-5663/

scribed in this work, due to its versatility and sensitivity. In the past few years, the IRIS system has been successfully used for quantification of DNA, protein adsorption on the surface, real-time monitoring of binding events, measuring binding rates, and as a quality control step in microarray fabrication (Sevenler et al., 2019; Zaraee et al., 2020). Since the IRIS system can provide label-free and multiplexed quantification of molecular binding events in real-time, it is a versatile technique for many applications including antibody development, environmental monitoring, and food quality control (Avci et al., 2015; Chiodi et al., 2020a; Sevenler et al., 2017; Seymour et al., 2021; Yurdakul et al., 2020).

In this study, protein A is immobilized on an IRIS chip as the ligand on the sensor, and surface characterization experiments are performed by ellipsometry, atomic force microscopy, and contact angle measurements in order to evaluate the homogeneity of the surface. Subsequently, the binding kinetics of IgG against protein A is measured using the IRIS system in the concentration range 1–50 μg/mL. Compared to the other techniques, this sensing system offers accurate, fast, easy, cost-effective, and sensitive sensing of IgG binding with protein A.

2. Materials and methods

2.1. Materials

Human immunoglobulin G (IgG) was purchased from Sigma Aldrich Corporation (St. Louis, MO, USA). The staphylococcal protein A (SpA; 42 kDa) was also obtained from Sigma Chemical Corporation (St. Louis, MO, USA) and reagents were kept at −20°C when not in use. Right before use, they were stored at 4°C. Other reagents were supplied from Merck A.G (Darmstadt, Germany) as an analytical and organic grade. Buffers and mediums were prepared with deionized water obtained from millipore Simplicity 185 Ultrapure Water System.

2.2. Sensing system and image analysis

The working principle of IRIS was widely described in literature (Aygun et al., 2017; Celebi et al., 2020; ~~Elisa et al., 2019~~; Sevenler et al., 2018). Briefly, the sensing method is based on measuring the change in optical path difference (OPD) on a thin film, as a result of biomass accumulation on a multi-layered sensor surface. A silicon/silicon dioxide (Si/SiO_2) layered substrate is used to prepare the microarray format sensors. An overview of the IRIS system was shown in Fig. 1. The optical setup is constituted by LEDs, an integrating sphere, a beam splitter, an objective, and a CMOS camera. In order to produce the IRIS signal, light from a partially coherent LED source is utilized to illuminate the chip surface, and the reflected light is collected through the same objective by a 50/50 beam splitter, and directed towards a CMOS-camera, in a common path interferometer configuration. Constructive interference of the light reflected by the $Si–SiO_2$ oxide interface and the SiO_2-immersion medium interface is achieved at certain wavelengths for a specifically engineered thickness of the oxide layer (100 nm) (Daaboul et al., 2011).

To perform the characterization experiments, the surface of the IRIS chip substrate is functionalized with capture probes for an analyte. Then, the microfluidic chamber is formed by assembling a thin pressure-sensitive adhesive gasket between an anti-reflective coated glass slide and the chip. Inlet and outlet laser—drilled holes on the two sides of the chip allow continuous flow through the fluidic chamber. Reflectance images are acquired from the assembled cartridge in the solution. During the binding experiments, the analyte solution was flowed across the surface of sensor at a constant speed of 50 μL/min, and the target molecules bind to the immobilized probes generating signals as they produce biomass accumulation (Fig. 2).

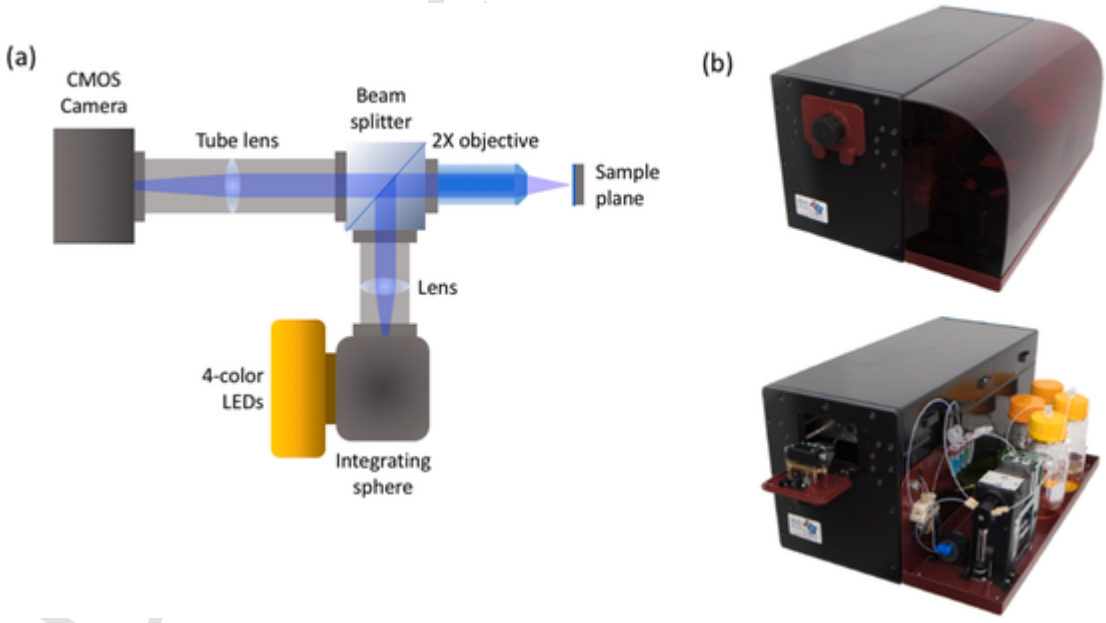

Fig. 1. Scheme of interferometer optical path (a) and photos of prototype IRIS instrument (b).Four-color low-coherence LEDs coupled with the integrating sphere are chosen as an illumination source to produce uniform illumination. The dominant wavelengths of the LEDs are red (λ_D = 630 nm), yellow (λ_D = 595 nm), green (λ_D = 525 nm) and blue (λ_D = 460 nm). Four-color images are taken as a calibration step at the beginning of the experiment to convert the brightness signal to mass-per-unit-area values (Sevenler and Ünlü, 2016). A 1.1″-inch format CMOS camera (FLIR BFS–U3–17S7M) is used for data collection. This low-magnification modality of IRIS provides a large, 5 mm × 7 mm field of view (FOV) using a 2X magnification objective with 0.06 numerical aperture (NA), making the technique very appealing for multiplexed applications. Recently, IRIS has evolved into a more powerful detection technology for label-free biomolecular interaction analysis with automated sample handling, and Python-based, user-friendly detection, and analysis software. (For interpretation of the references to color in this figure legend, the reader is referred to the Web version of this article.)

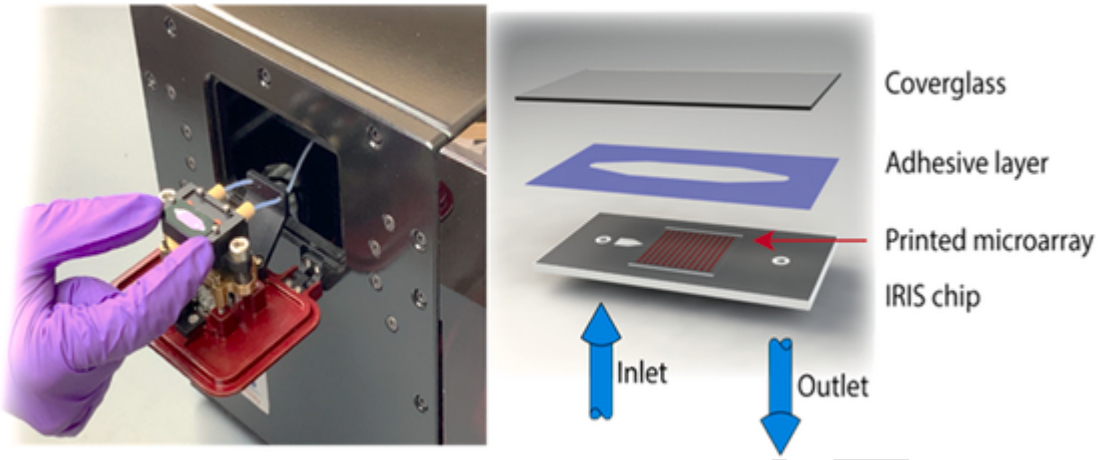

Fig. 2. IRIS microfluidic chamber and cartridge fixture with microfluidic connections.

2.3. Preparation of IRIS chip surfaces

As a first preliminary step, 3-(glycidoxypropyl)trimethoxysilane was used to produce an epoxy silane reactive coating on the surface of IRIS chips. The polymer was diluted in 100% isopropanol before use. The chips were then submerged in the epoxy silane solution for 3 min while gently swirling. Subsequently, they were rinsed in 100% isopropanol for 5 min and dried under a nitrogen stream for 1 h. Protein A and control protein (bovine serum albumin, BSA) were spotted onto the active chip at several concentrations (0.5, 0.75, 1.0, and 1.5 mg/mL) (Fig. 3). After spotting, the IRIS chips were left to incubate for 6 h at room temperature to allow protein binding. The spotted chip was treated with BSA %1 in phosphate buffer solution (PBS) for 5 min to deactivate the remaining polymer active binding sites, then quickly submerged in water and dried under the nitrogen stream.

2.4. Characterization of IRIS chip surfaces

The surface thickness of IRIS chips was characterized using ellipsometry (Nanofilm EP3). Auto-nulling imaging was utilized for measurements of all IRIS chips (bare, epoxy-modified, and protein A-immobilized surfaces). All measurements were obtained at a wavelength of 532 nm and 50° incidence angle. Atomic force microscopy (AFM, Asylum Research 3D Standalone) was also utilized as it provides the ability to perform measurements at high resolution due to the cantilever interferometer. The IRIS chips were placed in the microscope system by using a double-sided carbon strip and images were obtained with 256 × 256 pixels resolution on a 5 μm × 5 μm area. Observation studies were carried out via tapping mode in air. As a final characterization step, contact angle (KRUSS DSA100) measurements were performed with sessile drop method using water. The angle values were obtained from three separate measurements taken from different parts of surfaces and the average was calculated.

2.5. Detection of IgG with IRIS system

The real-time characterization of IgG was performed using protein A spotted IRIS chips in aqueous solutions. Kinetic data were acquired on the IRIS kinetics commercial system (iRiS Kinetics, Inc.). All the measurements were performed with the blue color LEDs (λ_D = 460 nm). First, equilibration buffer (PBS pH 7.4) was flown through the IRIS system at a 50 μL/min flow rate. Then, IgG solutions at various concentrations (1–50 μg/mL) were interacted across the surface of chip in the IRIS system. The changes in the mass-per-unit area were monitored in real-time. For all concentrations, a steady-state was reached after 120 s. Regeneration of chip surface was obtained by flowing 0.1 M glycerol-HCl solution, which caused desorption of bound IgG. The reusability of sensor chip was demonstrated by performing binding-regeneration cycles using same the IgG solution (10 μg/mL) 6 times.

3. Results and discussion

3.1. Characterization results

The surface thickness values of IRIS chips were measured as 20.2 ± 0.6 nm and 46.6 ± 1.4 nm for epoxy-modified and protein A-

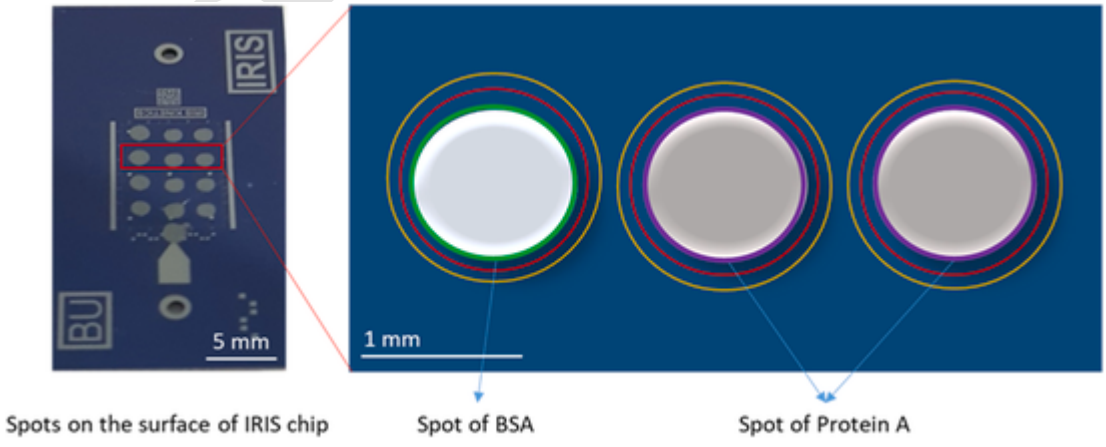

Fig. 3. Acquired images of spots on surface of IRIS chip.

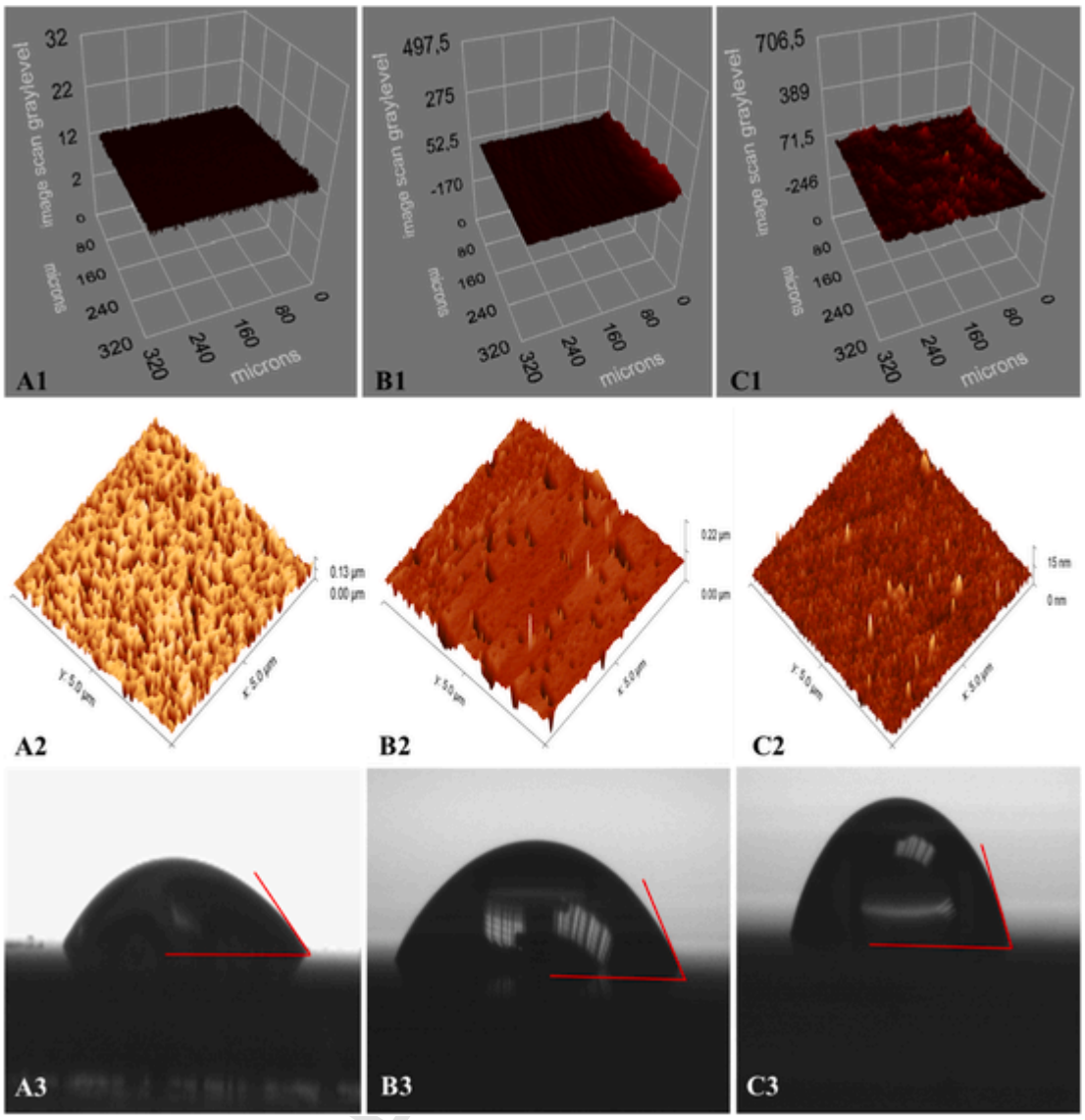

Fig. 4. Ellipsometry images of bare (A1), epoxy-modified (B1), and protein A-immobilized (C1) surfaces of IRIS chips; AFM images of bare (A2), epoxy-modified (B2), and protein A-immobilized (C2) surfaces of IRIS chips; and contact angle images of bare (A3), epoxy-modified (B3), and protein A-immobilized (C3) surfaces of IRIS chips.

immobilized surfaces with ellipsometry measurements, respectively. The thickness values indicated that the modification and immobilization of epoxy groups and protein A on the surface of IRIS chip was successfully achieved and the increase in the thickness of IRIS chip surface was shown in Fig. 4A1, 4B1, and 4C1. Furthermore, the root mean square (RMS) values of IRIS chips were measured as 22.96 ± 2.8 nm, 14.56 ± 3.6 nm, and 1.12 ± 0.2 nm for bare, epoxy-modified, and protein A-immobilized surface with AFM measurements. The decrease in the RMS values of IRIS chip surface was depicted in Fig. 4A2, 4B2, and 4C2, respectively. The contact angle of bare, epoxy-modified, and protein A-immobilized IRIS chip surfaces were determined as 28.6 ± 0.7, 54.6 ± 0.2, and 61.7 ± 0.5, respectively. As seen in Fig. 4A3, 4B3, and 4C3, the immobilization of protein A has indicated the hydrophobic properties, therefore, the hydrophobicity of the IRIS chip surface was increased.

3.2. Detection results of IgG

This study aims to design a rapid, simple, and sensitive technique for detection of IgG molecules in real-time. Protein A is a highly stable surface receptor with a molecular weight of 42 kDa. It can be produced by *Staphylococcus aureus* or by recombinant DNA technology. IgG has a basic four-chain monomeric structure, consisting of two identical heavy chains and two identical light chains with interchain disulfide bonds. It is known that Protein A has a high affinity for the F_c portion of IgG. Here, the IRIS system has successfully demonstrated high sensitivity, low-cost detection of IgG molecules binding kinetics using protein A as a ligand. The experimental studies were performed on IRIS chips functionalized in two different methods. The first category of chips was functionalized with different concentrations of protein A (*IRIS-proteinA1*). Several concentrations (0.5, 0.75, 1.0, and 1.5 mg/mL) of protein A were spotted on the IRIS chip surface to prepare *IRIS-proteinA1*, and the spots were labeled as PA1, PA2, PA3, and PA4. In this case, 0.1 mg/mL and 1.0 mg/mL IgG sample solutions were flown across the spotted chip for binding detection. As demonstrated in Fig. 5A and Fig. 5B, the increase in signal is correlated both to the increasing IgG concentration in solution as well as to the increasing concentration of protein A spots.

The second category of chips (*IRIS-proteinA2*) was prepared by spotting 1.5 mg/mL of protein A to obtain six identical spots on the chip

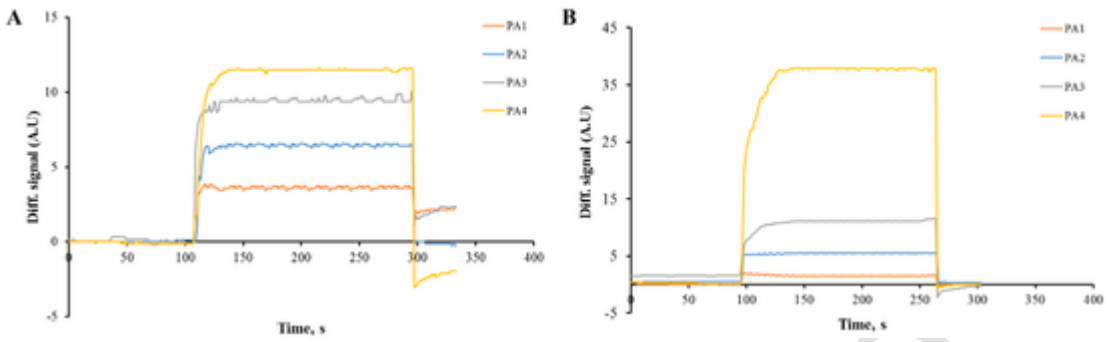

Fig. 5. Responses of IRIS-proteinA1 chip with different concentrations of protein A spotted for 0.1 mg/mL (A) and 1.0 mg/mL (B) IgG sample solutions.

surface. Following the chip preparation, IgG sample solutions at 1, 10, 20, 25, 30, and 50 μg/mL were flown across the chip surface. The signal responses of IRIS system were recorded and, as expected, the increase in signal level was correlated to the increase in IgG concentration (Fig. 6A). In order to verify repeatability, another experiment was performed on a single IRIS-proteinA2 chip by repeating a measurement at the same concentration of IgG (10 μg/mL) 6 times. The response of the system is shown in Fig. 6B, where the good overlap of the curves shows good repeatability of the binding-regeneration cycle. During the experimental procedure, the IRIS sensor surface was firstly equilibrated with PBS buffer (100 mM, pH 7.4) for 100 s, then the IgG solution was passed through the sensor surface for 100 s, the stable signals were monitored after 20 s passing IgG solution. This sensor system was offered many advantages in comparison to the standard detection methods. ELISA depended on the colorimetric method by using the enzyme-labeled antibodies is a widely adopted sensitive approach for the detection of antibodies; however, long incubation time, need for multi-washing step, and requirement of the labeled molecules are the main disadvantages for practical use of ELISA in clinical trials. The discrete steps are due to datatype selection with insufficient bit depth in the early version of the acquisition software, resulting in discretization noise hindering otherwise shot-noise-limited sensitivity of interferometric detection. While the datatype selection can be readily remedied, observed discretization noise does not affect the analysis and conclusions in this study.

The limit of detection (LOD) and limit of quantification (LOQ) of IRIS system was calculated according to Equations 1 and 2:

$$LOD = (3s)/b \quad (1)$$

$$LOQ = (10s)/b \quad (2)$$

where s is the standard deviation obtained from the calibration curve and b is the slope of the linear fit. The LOD and LOQ values were found to be 0.25 μg/mL (1.67 nM) and 0.83 μg/mL (5.51 nM). The data demonstrates that the combination of this system and the ligand at this concentration provide an effective method for sensitive detection of IgG.

We proceeded to analyze the acquired data. Generally, to fit binding kinetics data, the most common utilized models are Langmuir, Freundlich, and Langmuir-Freundlich isotherms (Levanr and Vermeulen, 1981). As these isotherm models characterize binding from subsequently diluted solutions, we can assume that the binding data acquired in this study are compatible with these isotherms when studied at mean concentration intervals. The graphics of isotherms were shown in Fig. 7.

The Langmuir isotherm considers a homogeneous surface. The chip surface needs to have the same number of active areas, as well as the same energy. This leads by approximation to the simplest theoretical model for binding/adsorption, the Langmuir model, described by the following equation.

$$T = [T_{max}\,(C) / K_D + (C)] \quad (7)$$

On the other hand, for heterogeneous surfaces, the Freundlich model is the first derived and most commonly applied model (Equation (8)).

$$T = [T_{max}\,(C)\ 1/n] \quad (8)$$

Here, T represents the sensor response, C is the concentration of IgG in the solution (μg/mL), K_D is the equilibrium dissociation constant. The association and dissociation equilibrium constants are shown with K_A (μg/mL)$^{-1}$ and K_D (μg/mL). In addition, the Freundlich exponent is defined by 1/n.

The Langmuir-Freundlich adsorption isotherm model is a useful model to investigate the binding behavior at high concentrations of the ligand and IgG molecules.

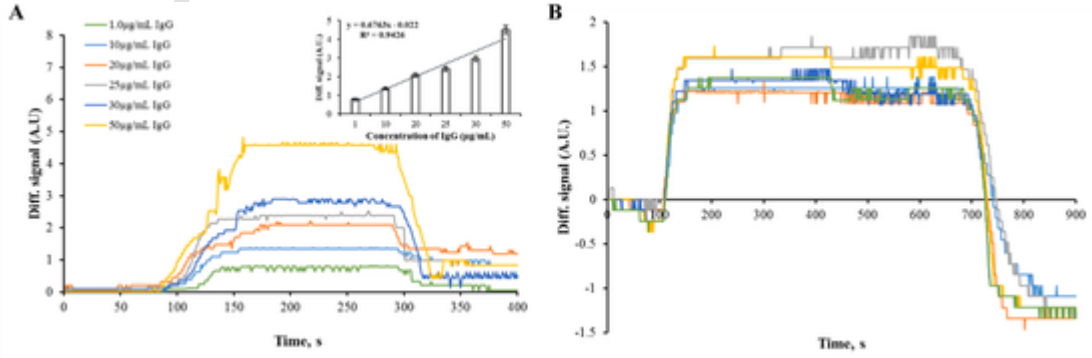

Fig. 6. Responses of IRIS-proteinA2 chip with the PA4 spot for IgG sample solutions (A) and reusability of IRIS-proteinA2 chip for IgG detection on each spot (B). Note that these binding curves have been acquired on a prototype IRIS instrument and the data shows discrete steps due to datatype selection in the early version of the acquisition software.

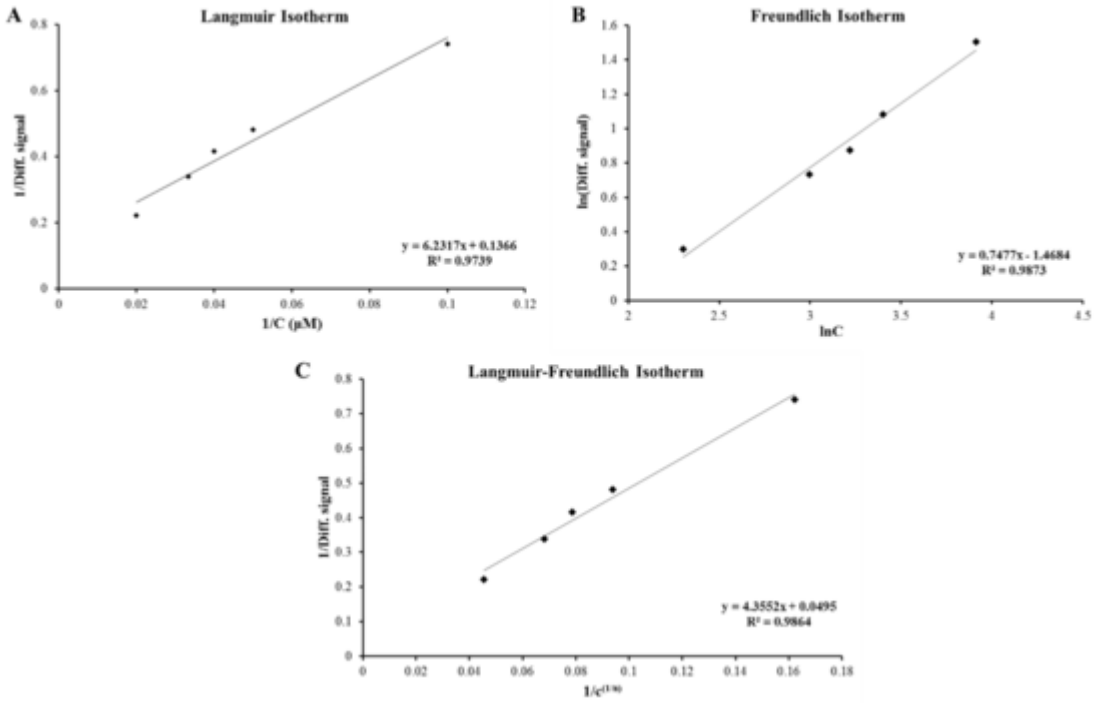

Fig. 7. Langmuir, Freundlich and Langmuir-Freundlich isotherms models applied to data acquired on IRIS chip.

$$T = [T_{max}\,(C)\,1/n / K_D + (C)\,1/n] \quad (9)$$

As depicted in Table 1, the results can be easily approximated to the Langmuir isotherm model with nearly T_{max} data, and by assuming that the sensor surface of IRIS chip was composed of a monolayer of probes with an equal number of binding sites per unit area. The comparison of IgG characterization with different methods was summarized in Table 2.

4. Discussion

The IRIS system is recognized as one of the most sensitive commercially available sensor technologies and has successfully been applied to binding kinetics measurements of a multitude of analytes, including small molecules, oligonucleotides, proteins, and antibodies, as well as to the detection of viruses and bacteria (Chiodi et al., 2020b). The IRIS system is suitable for early and direct recognition of biothreats, responding to the need for a real-time, fast, cost-effective, label-free, and precise biological characterization method (Cretich et al., 2012). In order to better understand the efficiency of IRIS system, it is possible to compare its performances to those of surface plasmon resonance sensor (SPR), one of the most widely utilized label-free sensors in the field of molecular characterization. SPR is a highly sensitive, flexible, and label-free characterization technique (Saylan et al., 2020). However, the measured binding data depends on environmental conditions, such as the refractive index of analyte solution, which changes with solvent addition, temperature, or pH. Moreover, in order to improve sensitivity and increase binding density, SPR utilizes a thick carboxymethylated dextran layer as its immobilization chemistry, making it susceptible to diffusion effects, which limit the kinetics of the binding reactions (Chiodi et al., 2021) and adversely affects the accuracy of affinity mea-

Table 1
Mathematical data of Langmuir, Freundlich and Langmuir-Freundlich isotherms of IRIS chip.

Langmuir		Freundlich		Langmuir-Freundlich	
T_{max}	7.35	T_{max}	3.1	T_{max}	20.4
K_A	1.18	1/n	0.74	1/n	0.0146
K_D	0.84	R^2	0.98	K_A	4.60
R^2	0.97			K_D	0.21
				R^2	0.98

Table 2
Comparison of IgG detection with different methods.

Type of sensor	Materials	Analyte	Concentration range	Limit of detection	Ref.
Surface plasmon resonance	Graphene oxide/ staphylococcal protein A co-modified tilted fiber	IgG	30–100 μg/mL	0.5 μg/mL	Wang et al. (2018)
Surface plasmon resonance	Polydopamine modified gold-film	Human-IgG	10–100 μg/mL	2 μg/mL	Shi et al. (2015)
Surface plasmon resonance	Gold-coated photonic crystal optical fiber	Anti-bovine IgG	1–20 mg/mL	267 μg/mL	Wong et al. (2013)
Surface plasmon resonance	Nanorods-Fe_3O_4 nanohybrids	Mouse IgG	0.15–40.00 μg/mL	0.15 μg/mL	Zhang et al. (2014)
Surface plasmon resonance	Silver nanocubes	Mouse IgG	2.50–40.00 μg/mL	0.6 μg/mL	Zhang et al. (2016)
L-surface plasmon resonance	Protein A-modified sensor chips	IgG	0.0015–10 mg/mL	0.0156 mg/mL	Tran et al. (2020)
Interferometric optical fiber	Single-mode fiber with large core-offset fusion splice	Human-IgG	0.5–5 μg/mL	2.3 ng/mL	Wang and Wang (2018)
Surface plasmon resonance	Gold nanoparticle-decorated graphene oxide	Rabbit IgG	0.1–50 μg/mL	0.1 μg/mL	Zhang et al. (2013)
IRIS sensor	Protein A-immobilized chip	Human IgG	1.0–50 μg/mL	0.25 μg/mL	**In this study**

surements (Drake et al., 2012). Here, we have demonstrated the ability of IRIS system to perform reliable IgG characterization with a monolayer of probes without being affected by the changes in detection medium.

A good example of the efficiency of IRIS system can be found in the literature is the allergen-specific IgE detection study. In this previous study, the clinical use of IRIS was demonstrated by detection of IgE from a microliter-sized sample, utilizing secondary antibodies against human IgE labeled with 40 nm gold nanoparticles (Monroe et al., 2011). The present study can be considered a follow-up of such work, since an improved version of the sensor is successfully applied to label-free, liquid, and real-time detection of IgG, in a sensitive, reliable, and fast manner. High sensitivity and specificity, no need for labeled reagents are the unique properties of this system for detection of molecules. In order to compare our results to previous studies that can be found in the literature, we have selected the most impactful papers where different sensor systems have been applied to the detection of IgG. For example, Wang et al. utilized a sensitive and novel graphene oxide-based SPR sensor using protein A to co-modify a tilted fiber Bragg grating, achieving highly sensitive detection of IgG. In this study, the gold surface of an SPR chip was modified with graphene oxide, and protein A was immobilized. The reported LOD value was around 0.5 μg/mL (Wang et al., 2018). In our study, we successfully designed a sensitive and inexpensive sensing system. In another study, Shi et al. utilized a method based on the adsorption of gold nanoparticles on the exposed surface of an optical fiber to sensitively bind IgG molecules. The reported LOD value was 2.0 μg/mL for IgG detection (Shi et al., 2015). Wong and their coworkers proposed a gold-coated photonic crystal optical fiber-based sensor as an SPR sensor. The sensor system was fabricated by collapsing the outputs of the fiber. Protein G was immobilized on the thiol-functionalized surface. They showed the ability of the sensor system to binding of the IgG with a LOD of 0.267 mg/L (Wong et al., 2013). We reported a low LOD value in our study without using any gold nanoparticles.

In the present study, we aimed to sensitively detect IgG molecules by binding them to protein A functionalized chips on IRIS system. Our limit of detection was determined to be 0.25 μg/mL, improved with respect to other studies reported in the literature. A summary of the alternative methods described in the literature to perform IgG detection is presented in Table 2. Here, IgG was selected as a model protein due to its crucial role in infectious diseases. The IRIS system has proven to offer a sensitive, reliable, multiplexed, and label-free optic technique with many advantages in comparison to the standard detection systems such as ELISA. ELISA is a well-established and highly selective method used in clinical studies. However, the lack of reusability of the ELISA kits, high cost, long preparation time, long analysis time due to multiple steps, and the requirement of agents like enzymatic, fluorescent, or chemiluminescent labels are the major drawbacks of this method. The IRIS system uses a highly scalable Si/SiO2 substrate, coupled with the low sample volume requirement decreases the cost of consumables drastically. The real-time detection enabled by this technology provides rapid results. Therefore, the time and cost per experiment are significantly reduced.

5. Conclusion

Rapid, sensitive, and reliable IgG detection and characterization are crucial for medical and diagnostics applications, due to the important role it plays as a biomarker for most infectious diseases. Because of the limitations of conventional detection techniques, the development of novel IgG sensing platforms has gained popularity. Here, the Interferometric Reflectance Imaging Sensor (IRIS) system is utilized to perform accurate and reliable IgG kinetic characterization measurements. Various binding kinetics experiments have been carried out in this study, and the performance of the imaging system is comprehensively evaluated. According to the results presented in the previous sections, the interferometry-based label-free sensor provides accurate, rapid measurements of IgG binding kinetics on a cost-effective platform. Furthermore, the IRIS system produces quantitative biomass accumulation results, showing potential for direct detection in clinical samples as a future perspective. In the light of the obtained data, the IRIS system represents a valid alternative to established methods such as SPR and ELISA for detection of relevant biomarkers in medical applications.

Funding

This work was partially funded by the Boston University Ignition Program and by the National Science Foundation Technology Translation Grant (NSF-TT PFI Award n1941195). The prototype IRIS instrument used in these studies has been developed under these grants.

Conflicts of interest

M.S.Ü. is the founder of a start-up company (iRiS Kinetics, Inc.) for the commercialization of the interferometric reflectance imaging sensor technique.

Uncited references

Oishi et al., 2003, Saylan and Denizli, 2018, Saylan et al., 2019

CRediT authorship contribution statement

Monireh Bakhshpour: Conceptualization, Methodology, Investigation, Validation, Formal analysis, Data curation, Writing – original draft, Writing – review & editing. **Elisa Chiodi:** Conceptualization, Methodology, Investigation, Writing – original draft, Writing – review & editing. **Iris Celebi:** Conceptualization, Methodology, Investigation, Writing – original draft, Writing – review & editing. **Yeşeren Saylan:** Investigation, Formal analysis, Data curation, Writing – original draft, Writing – review & editing. **Nese Lortlar Ünlü:** Methodology, Supervision, Writing – original draft, Writing – review & editing. **M. Selim Ünlü:** Methodology, Supervision, Writing – original draft, Writing – review & editing, Project administration, Funding acquisition, Resources. **Adil Denizli:** Supervision, Methodology, Writing – original draft, Writing – review & editing, Resources.

Declaration of competing interest

The authors declare that they have no known competing financial interests or personal relationships that could have appeared to influence the work reported in this paper.

References

Avci, O., Ünlü, N.L., Özkumur, A.Y., Ünlü, M.S., 2015. Sensors (Switzerland) 15, 17649–17665.
Aygun, U., Avci, O., Seymour, E., Urey, H., Ünlü, M.S., Ozkumur, A.Y., 2017. ACS Sens. 2, 1424–1429.
Bakhshpour, M., Derazshamshir, A., Bereli, N., Elkak, A., Denizli, A., 2016. Mater. Sci. Eng. C 61, 824–831.
Bakhshpour, M., Özgür, E., Bereli, N., Denizli, A., 2017. Colloids Surf., B 151, 264–270.
Bashal, F., 2013. Open Rheumatol. J. 7, 87–95.
Celebi, I., Geib, M.T., Chiodi, E., Ünlü, N.L., Kanik, F.E., Ünlü, M.S., 2020. Biosensors 10 (11), 158.
Chen, G., Wang, Yanmin, Qiu, L., Qin, X., Liu, H., Wang, X., Wang, Yanying, Song, G., Li, Fang, Guo, Y., Li, Fenjie, Guo, S., Li, Z., 2012. J. Proteonomics 75, 2824–2834.
Chiodi, E., Sola, L., Brambilla, D., Cretich, M., Marn, A.M., ÜnlÜ, M.S., Chiari, M., 2020a. Anal. Bioanal. Chem. 412 (14), 3477–3487.
Chiodi, E., Marn, A.M., Geib, M.T., Ekiz Kanik, F., Rejman, J., Ankrapp, D., Ünlü, M.S., 2020b. ACS Omega 5, 25358–25364.
Chiodi, E., Marn, A.M., Bakhshpour, M., Ünlü, N.L., Ünlü, M.S., 2021. Polymers.
Cretich, M., Monroe, M.R., Reddington, A., Zhang, X., Daaboul, G.G., Damin, F., Sola, L.,

Unlu, M.S., Chiari, M., 2012. Proteomics 12, 2963–2977.
Daaboul, G.G., Vedula, R.S., Ahn, S., Lopez, C.A., Reddington, A., Ozkumur, E., Ünlü, M.S., 2011. Biosens. Bioelectron. 26, 2221–2227.
Divya, K.P., Dharuman, V., 2021. Food Chem. 339, 127881.
Drake, A.W., Tang, M.L., Papalia, G.A., Landes, G., Haak-Frendscho, M., Klakamp, S.L., 2012. Anal. Biochem. 429, 58–69.
Hou, H., Wang, T., Zhang, B., Luo, Y., Mao, L., Wang, F., Wu, S., Sun, Z., 2020. Immunol. 9, 1–8.
Inci, F., Karaaslan, M.G., Mataji-Kojouri, A., Shah, P.A., Saylan, Y., Zeng, Y., Avadhani, A., Sinclair, R., Lau, D.T.Y., Demirci, U., 2020. Appl. Mater. Today. 20, 100709.
Kobayashi, N., Nagata, T., Shinagawa, S., Oka, N., Shimada, K., Shimizu, A., Tatebayashi, Y., Yamada, H., Nakayama, K., Kondo, K., 2013. Biochem. Biophys. Res. Commun. 430, 907–911.
Levanr, M.D., Vermeulen, T., 1981. Binary Langmuir 948, 3247–3250.
Monroe, M.R., Reddington, A.P., Collins, A.D., LaBoda, C., Cretich, M., Chiari, M., Little, F.F., Ünlü, M.S., 2011. Anal. Chem. 83 (24), 9485–9491.
Oishi, K., Inoue, S., Cinco, M.T.D.D., Dimaano, E.M., Alera, M.T.P., Alfon, J.A.R., Abanes, F., Cruz, D.J.M., Matias, R.R., Matsuura, H., Hasebe, F., Tanimura, S., Kumatori, A., Morita, K., Natividad, F.F., Nagatake, T., 2003. J. Med. Virol. 71, 259–264.
Peeling, R.W., Artsob, H., Pelegrino, J.L., Buchy, P., Cardosa, M.J., Devi, S., Enria, D.A., Farrar, J., Gubler, D.J., Guzman, M.G., Halstead, S.B., Hunsperger, E., Kliks, S., Margolis, H.S., Nathanson, C.M., Nguyen, V.C., Rizzo, N., Vázquez, S., Yoksan, S., 2010. Nat. Rev. Microbiol. 8, S30–S38.
Saylan, Y., Bereli, N., Uzun, L., Denizli, A., 2014a. Separ. Sci. Technol. 49 (10), 1555–1565.
Saylan, Y., Üzek, R., Uzun, L., Denizli, A., 2014b. J. Biomater. Sci. Polym. Ed. 25 (9), 881–894.
Saylan, Y., Denizli, A., 2018. Sensors, 18 Switzerland.
Saylan, Y., Akgönüllü, S., Yavuz, H., Ünal, S., Denizli, A., 2019. Sensors, 19 Switzerland.
Saylan, Y., Akgönüllü, S., Denizli, A., 2020. Biosensors 10 (10), 142.
Sevenler, D., Avci, O., Ünlü, M.S., 2017. Biomed. Opt Express 8, 2976.
Sevenler, D., Daaboul, G.G., Ekiz Kanik, F., Ünlü, N.L., Ünlü, M.S., 2018. ACS Nano 12, 5880–5887.
Sevenler, D., Ünlü, M.S., 2016. J. Mod. Opt. 63, 1115–1120.
Sevenler, D., Trueb, J., Ünlü, M.S., 2019. Proc. Natl. Acad. Sci. U. S. A. 116, 4129–4134.
Seymour, E., Ünlü, N.L., Carter, E.P., Connor, J.H., Ünlü, M.S., 2021. ACS Sens. 6, 229–237.
Shi, S., Wang, L., Su, R., Liu, B., Huang, R., Qi, W., He, Z., 2015. Biosens. Bioelectron. 74, 454–460.
Tran, T., Eskilson, O., Mayer, F., Gustavsson, R., Selegård, R., Lundström, I., Mandenius, C.F., Martinsson, E., Aili, D., 2020. Processes 8, 1–12.
Vidarsson, G., Dekkers, G., Rispens, T., 2014. Front. Immunol. 5, 1–17.
Wang, B.T., Wang, Q., 2018. Opt Commun. 426, 388–394.
Wang, Q., Jing, J.Y., Wang, B.T., 2018. IEEE Trans. Instrum. Meas. 68, 3350–3357.
Wong, W.C., Chan, C.C., Boo, J.L., Teo, Z.Y., Tou, Z.Q., Yang, H. Bin, Li, C.M., Leong, K.C., 2013. IEEE J. Sel. Top. Quant. Electron. 19.
Younes, N., Al-SAdeq, D.W., Al-Jighefee, H., Younes, S., Al-Jamal, O., Daas, H.I., Yassine, H.m., Nasrallah, G.K., 2020. Viruses 12, 582.
Yu, J., Zhang, Y., Zhang, Y., Li, H., Yang, H., Wei, H., 2016. Biosens. Bioelectron. 77, 366–371.
Yurdakul, C., Avci, O., Matlock, A., Devaux, A.J., Quintero, M.V., Ozbay, E., Davey, R.A., Connor, J.H., Karl, W.C., Tian, L., Ünlü, M.S., 2020. ACS Nano 14, 2002–2013.
Zaraee, N., Kanik, F.E., Bhuiya, A.M., Gong, E.S., Geib, M.T., Ünlü, N.L., Ozkumur, A.Y., Dupuis, J.R., Ünlü, M.S., 2020. Biosens. Bioelectron. 162, 112258.
Zhang, D., Sun, Y., Wu, Q., Ma, P., Zhang, H., Wang, Y., Song, D., 2016. Talanta 146, 364–368.
Zhang, Hua, Sun, Y., Gao, S., Zhang, Hanqi, Zhang, J., Bai, Y., Song, D., 2014. Talanta 125, 29–35.
Zhang, J., Sun, Y., Wu, Q., Zhang, H., Bai, Y., Song, D., 2013. Analyst 138, 7175–7181.